

FAME-ViL: Multi-Tasking Vision-Language Model for Heterogeneous Fashion Tasks

Xiao Han^{1,2} Xiatian Zhu^{1,3} Licheng Yu Li Zhang⁴ Yi-Zhe Song^{1,2} Tao Xiang^{1,2}

¹ CVSSP, University of Surrey ² iFlyTek-Surrey Joint Research Centre on Artificial Intelligence

³ Surrey Institute for People-Centred Artificial Intelligence ⁴ Fudan University

{xiao.han, xiatian.zhu, y.song, t.xiang}@surrey.ac.uk

lichengyu24@gmail.com lizhangfd@fudan.edu.cn

Abstract

In the fashion domain, there exists a variety of vision-and-language (V+L) tasks, including cross-modal retrieval, text-guided image retrieval, multi-modal classification, and image captioning. They differ drastically in each individual input/output format and dataset size. It has been common to design a task-specific model and fine-tune it independently from a pre-trained V+L model (e.g., CLIP). This results in parameter inefficiency and inability to exploit inter-task relatedness. To address such issues, we propose a novel **F**Ashion-focused **M**ulti-task **E**fficient learning method for **V**ision-and-**L**anguage tasks (**FAME-ViL**) in this work. Compared with existing approaches, **FAME-ViL** applies a single model for multiple heterogeneous fashion tasks, therefore being much more parameter-efficient. It is enabled by two novel components: (1) a task-versatile architecture with cross-attention adapters and task-specific adapters integrated into a unified V+L model, and (2) a stable and effective multi-task training strategy that supports learning from heterogeneous data and prevents negative transfer. Extensive experiments on four fashion tasks show that our **FAME-ViL** can save 61.5% of parameters over alternatives, while significantly outperforming the conventional independently trained single-task models. Code is available at <https://github.com/BrandonHanx/FAME-ViL>.

1. Introduction

A variety of real-world multi-modal, particularly Vision-and-Language (V+L) tasks exist in the fashion domain, including multi-modal recognition [44, 53, 61], multi-modal retrieval [21, 83] and image captioning [85]. The models developed for these tasks have been applied in diverse e-commerce applications, improving product discoverability, seller-buyer engagement, and customer conversion rate after catalogue browsing. Intrinsically, those V+L tasks are

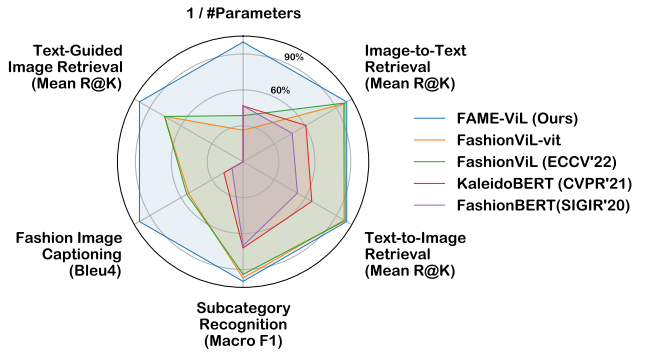


Figure 1. By multi-task learning a single model for heterogeneous fashion tasks, our **FAME-ViL** can significantly improve parameter efficiency, while boosting the model performance per task over existing *independently fine-tuned single-task models*. Note, each axis is **normalized** according to the respective maximum value for easier visualization.

heterogeneous in terms of (1) different input and output formats (e.g., text-guided garment retrieval [83] and image captioning [85] have completely different inputs and outputs); (2) different dataset sizes as the annotation difficulty of each task differ (e.g., the labeling effort for text-guided image retrieval is much harder than that for text-to-image retrieval [48, 83]).

Due to the heterogeneous nature of the V+L fashion tasks, existing methods [21, 24, 33, 87, 94] typically take a pre-trained generic V+L model [7, 38, 41–43, 49, 60, 67, 72, 79] and fine-tune it on every single task independently. Such an approach suffers from two limitations. (1) **Low parameter efficiency**: Each real-world application requires the deployment of its dedicated fine-tuned model, where there is no parameter or inference computation sharing. This leads to a linearly increasing storage and inference compute redundancy in the long run. (2) **Lack of inter-task relatedness**: Though the fashion tasks are heterogeneous

in nature, the fundamental components of the models are closely related in that all tasks require a deep content (image/sentence) understanding. Exploiting the shared information across tasks thus has the potential to improve model generalization capability leading to a performance boost.

Perhaps a natural solution would be applying Multi-Task Learning (MTL) [13]. However, most existing multi-task training methods [8, 36, 46, 56, 63] are designed for homogeneous tasks (*i.e.*, one dataset with multi-task labels) and thus cannot be directly applied to the heterogeneous fashion tasks. In our case, we are facing two challenges in building the fashion-domain MTL model: (1) *Architecturally*, it is non-trivial to model the diverse tasks in one unified architecture. Taking the popular CLIP [60] as an example, its two-stream architecture is designed for image-text alignment [52] and thus lacks the modality fusion mechanism as required by many V+L fashion tasks (*e.g.*, text-guided image retrieval [2, 83] and image captioning [85]). (2) In terms of *optimization*, a fashion-domain MTL model is prone to the notorious *negative transfer* problem [8, 13, 36, 46, 56, 63] due to both task input/output format differences and imbalanced dataset sizes. To the best of our knowledge, there has been no attempt at V+L MTL for the fashion domain.

In this work, we introduce a novel **F**ashion-focused **M**ulti-task **E**fficient learning method for various **V**ision-and-**L**anguage based fashion tasks, dubbed as **FAME-ViL**. It achieves superior performance across a set of diverse fashion tasks with much fewer parameters as in Fig. 1. Specifically, we design a task-versatile architecture on top of a pre-trained generic V+L model (*i.e.*, CLIP [60]). To adapt the simple two-stream architecture of CLIP to various fashion tasks, we introduce a lightweight *Cross-Attention Adapter (XAA)* to enable the cross-modality interaction between the two streams. It makes the model flexible to support multiple task modes (*e.g.*, contrastive mode for retrieval, fusion mode for understanding, and generative mode for generation). To address the negative transfer challenge, we introduce a *Task-Specific Adapter (TSA)* to absorb inter-task input/output format incompatibilities by introducing lightweight additional per-task parameters. For further handling the dataset imbalance problem, a *multi-teacher distillation* scheme [12] is formulated for our heterogeneous MTL problem. It leverages the pre-trained per-task teachers to guide the optimization of our multi-task model, mitigating the overfitting risks of those tasks with smaller training dataset sizes.

Our *contributions* are summarized as follows: **(I)** For the first time, we investigate the problem of multi-task learning on heterogeneous fashion tasks, eliminating the parameter redundancy and exploiting the inter-task relatedness. **(II)** We propose FAME-ViL with two novel adapters, adapting a pre-trained CLIP model to all tasks. **(III)** We introduce an efficient and effective multi-task training strategy sup-

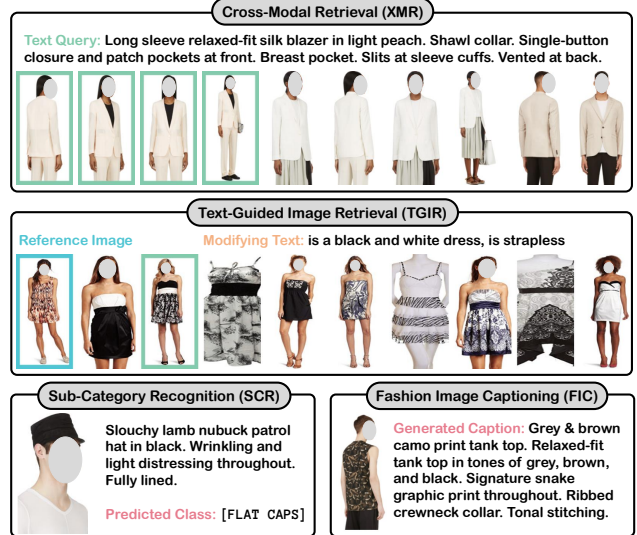


Figure 2. An illustration of four diverse fashion V+L Tasks studied in this work: cross-modal retrieval, text-guided image retrieval, sub-category recognition, and fashion image captioning. Note, all predictions shown in this figure are made by our FAME-ViL. Green box indicates the ground truth matches of retrieval tasks.

porting heterogeneous task modes in one unified model. **(IV)** Comprehensive experiments on four diverse fashion tasks (*i.e.*, cross-modal retrieval [52, 61], text-guided image retrieval [75, 83], multi-modal classification [61, 94], and image captioning [85]) show that our method significantly outperforms the previous single-task state-of-the-art with 61.5% parameter saving (see Fig. 1).

2. Related work

Vision-Language Pre-training (VLP). With the advent of Transformers [15, 17, 73], many pioneer studies [7, 31, 38, 41–43, 49, 67, 88] have demonstrated that VLP is effective in boosting various downstream V+L tasks in the generic domain. Since then, we have witnessed further developments of VLP methods, being bigger [19, 34, 60], more unified [50, 66, 77–79, 86] and more flexible [18, 76, 84].

Fashion V+L tasks. There exist a variety of heterogeneous tasks in the fashion domain. As depicted in Fig. 2, we consider four popular fashion tasks in this work: (1) *Cross-Modal Retrieval (XMR)* requests to efficiently retrieve the most matched image/sentence from a large candidate pool given a text/image query [52, 61]. (2) *Text-Guided Image Retrieval (TGIR)* is a special type of image retrieval with a multi-modal query (a combination of a reference image and a modifying text) matched against a set of images [6, 14, 23, 37, 39, 64]. It not only requires a strong fusion of the reference image and modifying text, but also an efficient matching between the fused representation and all candidate images [24, 83]. (3) *Sub-*

Category Recognition (SCR) requires an accurate class prediction made upon the fusion of an image-text pair [61, 94]. (4) *Fashion Image Captioning (FIC)* generates a caption to describe the given image with semantically meaningful, fine-grained, and accurate words [85]. Many recent works have been trying to address these fashion tasks through VLP [21, 22, 24, 33, 55, 87, 94]. Most of them focus on the pre-training, then simply fine-tune the pre-trained model on each downstream task independently. In contrast, we integrate all these tasks into a unified architecture and thus no separate fine-tuning is needed. Since our fashion data is also abundant, most early works pre-train on the fashion domain directly. However, a number of recent works [2, 3, 10, 16, 52] suggest that a generic-domain pre-trained CLIP [60] generalizes even better on the fashion tasks. In this work, we also exploit a pre-trained CLIP model. Different from the existing methods, we use a single multi-task learned model for all mentioned fashion tasks during fine-tuning.

Parameter-efficient tuning. Due to the increase in the size of V+L models, there is a growing interest in developing parameter-efficient methods to quickly adapt a large pre-trained model to specific tasks by using as few extra parameters as possible. The most representative methods are adapters [5, 9, 28, 70], prompt tuning [35, 47, 91, 92], low-rank adaptation [29] and their unified variants [25, 54, 89]. Interestingly, whilst MTL can save much larger parameters, it is under-studied in V+L modeling. In this work, we propose two kinds of adapters (XAA and TSA in Sec. 3.1) to adapt CLIP specifically designed for MTL in the fashion domain. Besides parameter-efficiently adapting CLIP, our proposed adapters also serve as the key component for task-versatile architecture design and enabling stable MTL.

Multi-task learning. Although MTL offers many advantages like improved data efficiency and reduced over-fitting, how to avoid negative transfer and cope with severely imbalanced dataset sizes is still an open question. One common solution is to weight per-task losses or combine per-task gradients into a joint update direction using various heuristics [8, 36, 46, 56, 63]. These works require the MTL model to have at least one forward propagation on each task so that they can manipulate the overall losses or gradients. However, since V+L tasks are typically heterogeneous (especially in the fashion domain), this requirement cannot be easily satisfied, making these methods not directly applicable. In contrast, Task Sampling-based MTL (TS-MTL) is without such a requirement and thus being widely adopted in V+L models [7, 30, 51, 57, 66]. In TS-MTL, only one task along with its data point is sampled per iteration. Since then, the heuristic task-sampling strategies [30, 32, 51] have been proposed, aiming to balance different tasks, avoiding the *over-fitting* on easier (or data-poor) tasks or *catastrophic forgetting* [20] on harder (or data-rich) tasks. However, it is found that TS-MTL on its own often underperforms single-

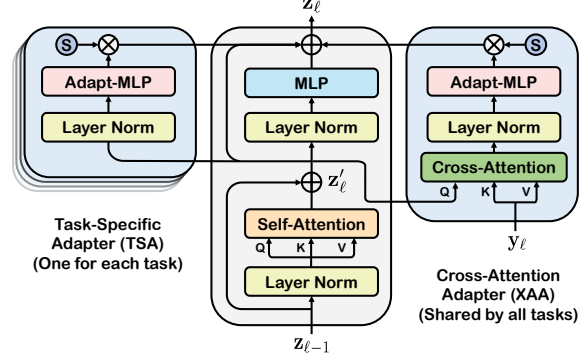


Figure 3. An illustration of a task-versatile Transformer layer equipped with two newly-introduced adapters: cross-attention adapter (XAA) and task-specific adapter (TSA).

task trained models; it is thus typically followed by an additional per-task fine-tuning step [30, 51]. In this work, we formulate an effective knowledge distillation with multiple single-task teachers [12] to alleviate the negative transfer without further fine-tuning on each task.

3. Methodology

We aim to address the most popular fashion tasks (shown in Fig. 2) using one single unified model. We introduce the details of our proposed FAME-ViL as follows.

3.1. Model architecture

FAME-ViL consists of a language encoder and a vision encoder initialized from the pre-trained CLIP (ViT-B/16 version) [60], as well as a set of newly introduced adapters. **Transformer layers.** The key component in CLIP is the transformer backbone [17, 73]. A vanilla Transformer encoder consists of an input embedding layer (word embedding for language input and patch embedding for vision input) and several alternating layers made of Multi-Head Self-Attention (MHSA) and MLP blocks. Layer Normalization (LN) [1] is applied before every block, and residual connections after every block [17, 60]. As shown in the middle of Fig. 3, this process can be formulated as follows:

$$\mathbf{z}_0 = \text{Embedding}(\mathbf{x}), \quad \mathbf{z}_0 \in \mathbb{R}^{N \times D}, \quad (1)$$

$$\mathbf{z}'_\ell = \text{MHSA}(\text{LN}(\mathbf{z}_{\ell-1})) + \mathbf{z}_{\ell-1}, \quad \ell = 1 \dots L, \quad (2)$$

$$\mathbf{z}_\ell = \text{MLP}(\text{LN}(\mathbf{z}'_\ell)) + \mathbf{z}'_\ell, \quad \ell = 1 \dots L, \quad (3)$$

where N, D, L denotes the number of input tokens, transformer dimension, and the number of layers, respectively.

Proposed adapters. To adapt the original Transformer layers in CLIP to different fashion downstream tasks, we design two kinds of adapters in architecture design: (1) Task-Specific Adapter (TSA) for accommodating the non-shareable characteristics of each individual task (Fig. 3 left);

(2) Cross-Attention Adapter (XAA) for enabling the interaction between different modalities (Fig. 3 right).

For TSA we adopt the scaled parallel adapter [5, 25] that adds another bottleneck MLP (AdaptMLP) in parallel with the original MLP of each transformer layer. Given an immediate input \mathbf{z}'_ℓ , it produces the adapted features, \mathbf{z}_ℓ^{tsa} , via:

$$\mathbf{z}_\ell^{tsa} = s \cdot \text{AdaptMLP}(\text{LN}(\mathbf{z}'_\ell)), \quad (4)$$

where s represents a learnable scale.

We construct an XAA module by further adding another Multi-Head Cross Attention (MHXA) layer [18, 49, 72] at the bottom of a TSA. Specifically, this MHXA uses the hidden state of the current stream \mathbf{z}'_ℓ as the queries and the output \mathbf{y}_ℓ (e.g., hidden state after MHSA or MLP) of another stream as the keys and values. The attended cross-modality features \mathbf{z}_ℓ^{xaa} are computed via:

$$\mathbf{z}_\ell^{xaa} = s \cdot \text{AdaptMLP}(\text{LN}(\text{MHXA}(\mathbf{z}'_\ell, \mathbf{y}_\ell))). \quad (5)$$

Within this mechanism, our XAA can exchange the information between different modalities.

Finally, both \mathbf{z}_ℓ^{tsa} and \mathbf{z}_ℓ^{xaa} are added up to the original output via residual connections. We thus rewrite Eq. (3) as:

$$\mathbf{z}_\ell = \text{MLP}(\text{LN}(\mathbf{z}'_\ell)) + \mathbf{z}'_\ell + \mathbf{z}_\ell^{tsa} + \epsilon \cdot \mathbf{z}_\ell^{xaa}, \epsilon \in \{0, 1\}, \quad (6)$$

where ϵ represents a gate that can turn on/off XAA according to the task need.

Operational modes and fashion tasks. Our FAME-ViL can switch among three operational modes to flexibly support various fashion tasks (see Fig. 4).

◊ **Contrastive mode:** This mode supports *Cross-Modal Retrieval* (XMR) tasks, including both text-to-image and image-to-text retrieval [24, 52]. All XAA modules are turned off as no need for inter-modal interaction, whereas only TSA modules are applied as in Fig. 4(a). During training, given a batch of B image-text pairs $(\mathbf{I}, \mathbf{T}) = \{(I_1, T_1), \dots, (I_B, T_B)\}$, we first compute their unimodal representations by the TSA-equipped vision and language encoders independently. Then, we maximize their similarities via symmetrical contrastive loss:

$$\mathcal{L}_{\text{XMR}} = \frac{1}{2} [\mathcal{L}_{\text{InfoNCE}}(\mathbf{T}, \mathbf{I}) + \mathcal{L}_{\text{InfoNCE}}(\mathbf{I}, \mathbf{T})], \quad (7)$$

$$\mathcal{L}_{\text{InfoNCE}}(\mathbf{X}, \mathbf{Y}) = -\frac{1}{B} \sum_{i=1}^B \log \frac{\exp(s(X_i, Y_i)/\tau)}{\sum_{j=1}^B \exp(s(X_i, Y_j)/\tau)}, \quad (8)$$

where τ is a learnable temperature. The similarity is measured by the dot product of their pooled then normalized features: $s(I_i, T_j) = f_\theta^{[c]}(I_i)^T \cdot f_\theta^{[c]}(T_j)$.

◊ **Fusion mode:** As in Fig. 4(b), both XAA and TSA modules are enabled in this mode. Given an input image-text pair (I, T) , the model serves as a single-stream fusion encoder producing two cross-modal attended representations: $f_\theta^{[f]}([I; T])$ and $f_\theta^{[f]}([T; I])$. The final fused representation is a simple addition: $f_\theta^{[f]}(I, T) = f_\theta^{[f]}([I; T]) +$

$f_\theta^{[f]}([T; I])$ ¹. This mode is useful for the *Sub-Category Recognition* (SCR) [61, 94] and *Text-Guided Image Retrieval* (TGIR) [75, 83].

SCR aims to predict the subcategory of fashion products based on both input image and text. We thus append a classifier on top of the fused representation and minimize its cross-entropy loss:

$$\mathcal{L}_{\text{SCR}} = -\mathbb{E}_{(I, T) \sim D} \log P(f_\theta^{[f]}(I, T)). \quad (9)$$

Considering the unique challenges of TGIR (i.e., requiring not only strong fusion but also efficient matching), FAME-ViL operates in a hybrid mode for it. Formally, given a batch of {reference images \mathbf{I}^r , modifying text \mathbf{T} , target images \mathbf{I}^t }, we first calculate the fused representation $f_\theta^{[f]}(\mathbf{I}^r, \mathbf{T})$ in the fusion mode; Then, we obtain the target image representation $f_\theta^{[c]}(\mathbf{I}^t)$ in the contrastive mode. During training, we pull them closer in a contrastive way:

$$\mathcal{L}_{\text{TGIR}} = \mathcal{L}_{\text{InfoNCE}}((\mathbf{I}^r, \mathbf{T}), \mathbf{I}^t), \quad (10)$$

where the similarity is still measured by dot product:

$$s((I_i^r, T_i), I_j^t) = f_\theta^{[f]}(I_i^r, T_i)^T \cdot f_\theta^{[c]}(I_j^t).$$

◊ **Generative mode:** This works as a seq2seq model performing the generative tasks auto-regressively [11, 71], e.g., *Fashion Image Captioning* (FIC) [85]. As in Fig. 4(c), we use a TSA-equipped vision encoder as the encoder, a TSA-equipped language encoder as the decoder, and only image-to-text XAA modules for the conditional caption synthesis. Following a standard encoder-decoder architecture, our image encoder provides *layer-wise* latent memory and the text decoder learns to maximize the conditional likelihood of the paired text under the forward auto-regressive factorization [40, 86]:

$$\mathcal{L}_{\text{FIC}} = -\mathbb{E}_{(I, T) \sim D} \sum_{a=1}^A \log P(T_a | f_\theta^{[g]}(I; T_{<a})), \quad (11)$$

where A denotes the length of each sentence, and $f_\theta^{[g]}([I; T])$ denotes the representation. During training, we enforce the teacher forcing [81] to achieve parallel computation and thus maximize the learning efficiency.

3.2. Heterogeneous multi-task learning

For training \mathcal{T} fashion tasks, we need to optimize both task-agnostic parameters θ_s (i.e., CLIP backbone & XAA modules) and a set of task-specific components $\{\theta_t\}_{t=1}^{\mathcal{T}}$ (i.e., TSA modules & task heads). Our objective is to maximize the overall performance across all tasks. The heterogeneity nature of fashion tasks causes the discrepancy in

¹More complex fusion methods (e.g., [2]) may yield better results. We leave this for future study.

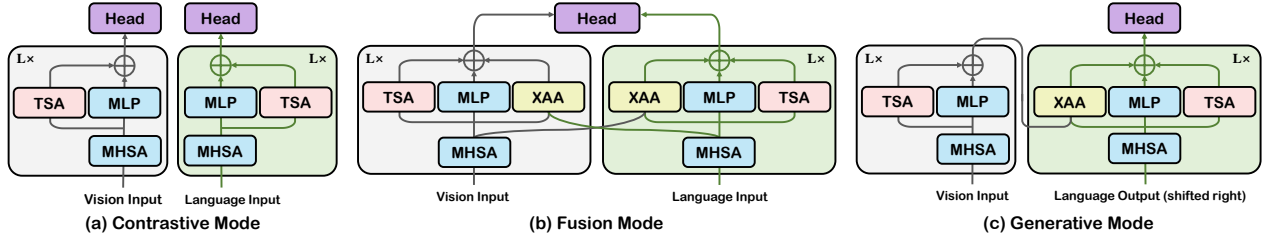


Figure 4. Schematic overview of three operational modes with our FAME-ViL. XAA: Cross-Attention Adapter; TSA: Task-Specific Adapter. Layer normalization and original residual connections are not shown here for simplicity.

mini-batch construction and training dynamics (*e.g.*, converging speed, overfitting) as well as data imbalance, making our multi-task learning particularly challenging. To address all these issues, we exploit the idea of Multi-Teacher Distillation (MTD) [12, 27].

Specifically, MTD consists of two stages. In the *first stage*, we train a teacher model with the identical architecture as our multi-task model on every task. Then in the *second stage*, we apply these teachers to guide the training of the multi-task model (*i.e.*, the student) with designed per-task distillation objectives.

For XMR, we first compute the image-text similarity using the features of the single-task teacher g_{xmr} : $\tilde{s}(I_i, T_j) = g_{\text{xmr}}(I_i)^T \cdot g_{\text{xmr}}(T_j)$. Using this similarity as a pseudo-target, we maximize its mutual information with the student’s counterpart [41]:

$$\mathcal{L}_{\text{XMR}}^{\text{D}} = \frac{1}{2B} \sum_b (\text{KL}(s_{b,\cdot} \parallel \tilde{s}_{b,\cdot}) + \text{KL}(s_{\cdot,b} \parallel \tilde{s}_{\cdot,b})), \quad (12)$$

where $\text{KL}(\cdot \parallel \cdot)$ denotes the Kullback–Leibler divergence loss on the softmax of the inputs.

For TGIR, we use a similar method as XMR to distill the knowledge from single-task teacher g_{tgir} :

$$\mathcal{L}_{\text{TGIR}}^{\text{D}} = \frac{1}{B} \sum_b \text{KL}(s_{(b,b),\cdot} \parallel \tilde{s}_{(b,b),\cdot}), \quad (13)$$

where the soft target is calculated via: $\tilde{s}((I_i^r, T_i), I_j^t) = g_{\text{tgir}}(I_i^r, T_i)^T \cdot g_{\text{tgir}}(I_j^t)$.

For SCR and FIC, we directly use the classification probabilities predicted by the teachers as pseudo-targets:

$$\mathcal{L}_{\text{SCR}}^{\text{D}} = \text{KL}(f_{\theta}^{[f]}(I, T) \parallel g_{\text{scr}}(I, T)), \quad (14)$$

$$\mathcal{L}_{\text{FIC}}^{\text{D}} = \sum_{a=1}^A \text{KL}(f_{\theta}^{[g]}(I; T_{<a})_a \parallel g_{\text{fic}}(I; T_{<a})_a). \quad (15)$$

Task scheduling. For training simplicity, we randomly sample one task per iteration. We optimize the summation of the original loss and distillation loss as:

$$\mathcal{L} = \mathcal{L}_{[\text{task}]} + \mathcal{L}_{[\text{task}]}^{\text{D}}, \quad [\text{task}] \sim \{\text{XMR}, \text{TGIR}, \text{SCR}, \text{FIC}\}, \quad (16)$$

where P denotes the sampling probability. To tackle data imbalance, unless stated otherwise we set the sampling probability for a particular task τ linearly proportional to the size of its dataset $|D_{\tau}|$ [30, 62]. We name this strategy as *size-proportional sampling*.

4. Experiments

Datasets. We evaluate our model on the datasets commonly used in the previous methods. Specifically, we test FashionGen [61] for XMR, SCR, and FIC, and FashionIQ [83] for TGIR. FashionGen [61] contains 68k fashion products accompanied by text descriptions. Each product includes 1 ~ 6 images from different angles, resulting in 260.5k image-text pairs for training, and 35.5k for testing. FashionIQ contains 18k training triplets (*i.e.*, reference image, modifying text, target image) and 6k validation triplets over three categories: Dress, Shirt, and Tootie. Each pair (reference image, target image) is manually annotated with two modifying texts, which are concatenated [83].

Implementation details. We use MMF [65] and PyTorch [59] to implement our FAME-ViL. We use the off-the-shelf CLIP from HuggingFace [82] as our pre-trained model. We use 4 RTX 3090 GPUs for the multi-task training. The default bottleneck dimension of AdaptMLP is 64. More implementation details are listed in the supplementary file.

Performance metrics. Following [24, 94], we report R@K for retrieval, Accuracy & Macro F_1 for classification and BLEU-4 [58] & METEOR [4] & ROUGE-L [45] & CIDEr [74] for captioning. (1) For each task, we first report *the average absolute performance*: $\mu_{\mathcal{T}_i} = \frac{1}{|M|} \sum_{j=0}^{|M|} M_{\mathcal{T}_i,j}$. (2) Since there is no unified objective among multiple tasks and the scale of per-task metrics often varies largely, we then report *the average per-task relative performance* $\Delta_{\mathcal{T}_i}$ w.r.t. the single-task baseline: $\Delta_{\mathcal{T}_i} = (\mu_{\mathcal{T}_i} - \mu_{\text{STL}}) / \mu_{\text{STL}}$. This can clearly indicate the positive/negative transfer effect. (3) We also report *the relative parameters saving* of FAME-ViL and its variants w.r.t. the vanilla CLIP baseline. Note, inference speed comparison is infeasible as this depends on the application of different tasks (no fixed rules).

Methods	Image to Text			Text to Image			Mean
	R@1	R@5	R@10	R@1	R@5	R@10	
FashionBERT [21]	23.96	46.31	52.12	26.75	46.48	55.74	41.89
OSCAR [43]	23.39	44.67	52.55	25.10	49.14	56.68	41.92
KaleidoBERT [94]	27.99	60.09	68.37	33.88	60.60	68.59	53.25
EI-CLIP [52]	38.70	72.20	84.25	40.06	71.99	82.90	65.02
MVLT [33]	33.10	77.20	91.10	34.60	78.00	89.50	67.25
FashionViL [24]	65.54	91.34	96.30	61.88	87.32	93.22	82.60
FashionViL(vit)	63.74	90.02	95.98	60.76	86.18	92.96	81.61
FAME-ViL(ST)	65.02	90.96	96.20	63.56	86.84	93.06	82.61
FAME-ViL	65.94	91.92	97.22	62.86	87.38	93.52	83.14

Table 1. Cross-Modal Retrieval (XMR) results on FashionGen [61]. Test protocol: random 100 [21, 24, 94].

4.1. Comparisons with prior art methods

We compare our models with the previous state-of-the-art methods on each task. For extensive and fair comparisons, all the prior competitors are based on large-scale pre-trained models. We even implement an enhanced variant of the latest art model FashionViL [24] by replacing ResNet50 [26] with the ViT-B/16 [17] backbone (same as our FAME-ViL), denoted as FashionViL(vit). In design, all the previous methods adopt Single-Task Learning (STL). We compare them with two variants of our model: (1) single unified MTL model; (2) STL variant of our FAME-ViL, denoted as FAME-ViL(ST), which is trained on each task independently using the same TSA and XAA design as FAME-ViL.

XMR evaluation. We consider both image-to-text retrieval and text-to-image retrieval with two kinds of protocols used by previous methods: (1) random 100: For each query, 100 candidates are randomly sampled from the same category to construct a retrieval database; The goal is to locate the positive match depicting the same garment instance from these 100 same-category negative matches [21, 33, 94]. (2) full database: We also adopt a more challenging and practical protocol that conducts retrieval on the entire product set [24, 52], which is in line with actual product retrieval scenarios. We use random 100 to compare with prior art methods while using full database to do ablation studies. The results of XMR on FashionGen [61] are reported in Tab. 1. We draw several observations: (1) Our FAME-ViL outperforms all prior art fashion models often by a large margin, validating the performance advantages of our method over alternatives in addition to better parameter efficiency. (2) FAME-ViL is superior over its single-task variant FAME-ViL(ST) in most cases and on the average accuracy, suggesting that our multi-task learning strategy is effective in exploiting the inter-task relatedness. (3) Our FAME-ViL(ST) can surpass all prior models pre-trained on large fashion domain data [21, 24, 43, 94], suggesting that using fashion data in pre-training is not necessarily most important, and model design (e.g., our TSA and XAA) could play a more significant role. Similarly, its large margin over

Methods	Dress		Shirt		Toptee		Mean
	R@10	R@50	R@10	R@50	R@10	R@50	
CIRPLANT [48]	17.45	40.41	17.53	38.81	21.64	45.38	30.20
TIRG(bert) [75]†	27.17	53.25	22.28	45.58	27.84	57.11	38.87
FashionVLP [22]	26.77	53.20	22.67	46.22	28.51	57.47	39.14
FashionViL [24]	33.47	59.94	25.17	50.39	34.98	60.79	44.12
FashionViL(vit)	31.53	57.91	26.74	50.69	36.77	61.81	44.24
Baldrati et al. [2]	33.81	59.40	39.99	60.45	41.41	65.37	50.07
Zhao et al. [90]	33.60	58.90	39.45	61.78	43.96	68.33	51.00
FAME-ViL(ST)	37.78	63.86	45.63	66.78	47.22	70.88	55.36
FAME-ViL	42.19	67.38	47.64	68.79	50.69	73.07	58.29

Table 2. Text-Guided Image Retrieval (TGIR) results on FashionIQ [83]. †: The results taken from [24].

Methods	SCR			FIC				
	Acc	F ₁	Mean	B	M	R	C	Mean
FashionBERT [21]†	85.27	62.00	73.64	3.30	9.80	29.70	30.10	18.23
OSCAR [43]†	84.23	59.10	71.67	4.50	10.90	30.10	30.70	19.05
KaleidoBERT [94]	88.07	63.60	75.84	5.70	12.80	32.90	32.60	21.00
FashionViL [24]	92.23	83.02	87.63	16.71	25.97	37.82	39.08	29.90
MVLT [33]	93.57	82.90	88.24	-	-	-	-	-
FashionViL(vit)	94.01	85.77	89.89	16.18	25.60	37.23	39.30	29.58
FAME-ViL(ST)	94.33	86.21	90.27	29.97	24.83	54.79	145.1	63.67
FAME-ViL	94.67	88.21	91.44	30.73	25.04	55.83	150.4	65.50

Table 3. Results of Subcategory Recognition (SCR) and Fashion Image Captioning (FIC) on FashionGen [61]. †: copied from [94].

the previous pre-trained CLIP-based model [52] further validates the significance of model architecture design.

TGIR evaluation. We compare our FAME-ViL with TGIR-specialist methods [2, 22, 48, 75, 90] and the art fashion-focused V+L model FashionViL [24] under the original protocol used by FashionIQ [83]. The results are given in Tab. 2. We have similar observations as on XMR. In particular, we note that our single-task variant already achieve a new art performance. With a simple addition-based fusion mechanism, FAME-ViL can even outperform significantly [2] with the same CLIP pre-training and a complex fusion module. We attribute this mostly to the contribution of XAA-backed inter-modal interaction (See Tab. 4).

SCR evaluation. We report the performance of SCR in the left part of Tab. 3, following the common protocol [21, 24, 94]. Similar to TGIR, our FAME-ViL surpasses clearly all previous works [21, 24, 33, 43, 94] with heavier fusion mechanisms (e.g., modality-agnostic self-attention implemented by concatenating text tokens and image patches at the very beginning). This validates the efficacy of our proposed XAA, suggesting the superiority of modality interaction over the conventional fusion at the input point.

FIC evaluation. The original FashionViL [24] has no decoder and cannot support generation tasks. For comparison, we equip it with masked language modelling (MLM) autoregressively [43, 93, 94] enabling the image captioning. The results of FIC are shown in the right part of Tab. 3, following the common protocol [94]. Our FAME-ViL again achieves state-of-the-art performance with a clear margin.

Groups	Methods	#Params (%)	\mathcal{T}_1 : XMR		\mathcal{T}_2 : TGIR		\mathcal{T}_3 : SCR		\mathcal{T}_4 : FIC		$\bar{\mu}$	$\bar{\Delta}$
			μ	Δ	μ	Δ	μ	Δ	μ	Δ		
I (Sec. 4.2)	(1) STL	0.0	66.30	0.0	51.87	0.0	90.34	0.0	-	-	52.13	0.0
	(2) STL + TSA	+1.35	69.99	+5.56	52.59	+1.39	90.10	-0.27	-	-	53.25	+1.67
	(3) STL + XAA	+14.70	66.30	0.0	53.83	+3.78	89.89	-0.50	63.70	0.0	68.43	+0.82
	(4) STL + TSA + XAA (FAME-ViL(ST))	+15.96	69.99	+5.56	55.47	+6.94	90.27	-0.07	63.67	-0.05	69.85	+3.10
II (Sec. 4.2)	(5) MTL	-70.43	57.65	-13.05	49.57	-4.43	85.95	-4.86	-	-	48.29	-5.59
	(6) MTL + TSA	-70.11	67.97	+2.52	52.04	+0.33	90.32	-0.02	-	-	52.58	+0.71
	(7) MTL + XAA	-67.65	65.87	-0.65	52.59	+1.39	90.93	+0.65	60.99	-4.25	67.60	-0.72
	(8) MTL + TSA + XAA (base MTL)	-67.33	69.31	+4.54	55.41	+6.82	90.84	+0.55	65.17	+2.31	70.18	+3.56
III (Sec. 4.3)	(9) base MTL + MTD (FAME-ViL)	-67.33	70.00	+5.56	58.29	+12.38	91.44	+1.22	65.50	+2.83	71.31	+5.50
	(10) base MTL + MTD + Uniform	-67.33	67.70	+2.11	57.31	+10.49	91.36	+1.13	65.12	+2.23	70.37	+3.99
	(11) base MTL + MTD + Round-robin	-67.33	67.79	+2.25	57.47	+10.80	91.35	+1.12	64.87	+1.84	70.37	+4.00
	(12) base MTL + IAS [32]	-67.33	69.13	+4.27	55.26	+6.54	90.51	+0.19	63.67	-0.05	69.64	+2.74
	(13) base MTL + MTD + IAS [32]	-67.33	70.11	+5.75	57.97	+11.76	90.88	+0.60	65.66	+3.08	71.16	+5.30
	(14) base MTL + IMTLG [46]	-67.33	64.11	-3.30	47.12	-9.16	90.21	-0.14	55.61	-12.70	64.26	-6.33
	(15) base MTL + MTD + IMTLG [46]	-67.33	67.14	+1.27	57.22	+10.31	90.09	-0.28	58.14	-9.56	68.15	+0.44
IV (Sec. 4.4)	(16) FAME-ViL (bottleneck dim. = 128)	-65.14	70.73	+6.68	58.03	+11.88	91.54	+1.33	66.20	+3.92	71.63	+5.95
	(17) FAME-ViL (bottleneck dim. = 256)	-62.67	71.77	+8.25	58.45	+12.69	91.10	+0.84	66.81	+4.88	72.03	+6.67
	(18) FAME-ViL (bottleneck dim. = 512)	-57.73	72.32	+9.08	58.51	+12.80	90.96	+0.69	66.92	+5.05	72.18	+6.91

Table 4. Ablation study and further analysis of our method. Groups (I) and (II): Ablation experiments of the proposed XAA and TSA under the single-task learning (STL) and multi-task learning (MTL) scenarios. Group (III): The comparison among our multi-teacher distillation (MTD) and other alternatives designed for task-sampling based MTL (TS-MTL). Group (IV): The effect of the bottleneck dimension of XAA and TSA. **Yellow background**: The baseline performance used per column; **Red background**: negative transfer; **Green background**: positive transfer. **Bold number**: The best result in each group.

All the above comparisons show the superior generalization capability of our method in both generative and discriminative tasks.

4.2. Ablation study on architecture

Given the strong performance of our method as evaluated in Sec. 4.1, we ablate the proposed model architecture with a focus on two newly introduced adapters (TSA and XAA) in both STL and MTL settings.

Single-task learning setting. For comparison on XMR, TGIR and SCR, we design the baseline as directly fine-tuning the vanilla CLIP without any new modules (L1). With the two-stream design, CLIP cannot tackle FIC, and we hence further equip it with our XAA as the baseline for FIC (L3). From the results shown in group (I) of Tab. 4, we find that TSA and XAA can bring in 3%-6% relative improvements for XMR and TGIR. In particular, XAA gives TGIR a significant improvement, demonstrating the superiority of our layer-wise modality interaction mechanism. However, these adapters have only a marginal impact on the performance of SCR and FIC, with a performance drop of less than 0.5% when the model is independently trained on a single task.

Multi-task learning setting. Similarly, we construct the baselines for the MTL setting using the vanilla CLIP and XAA-equipped CLIP (L5 and L7). As shown in L5 in the group (II) of Tab. 4, a severe negative transfer occurs with an overall 5.59% performance drop. Likewise, there is also a negative transfer for the XAA-equipped CLIP model (L7), albeit with a slight increase in performance. This sug-

gests the challenges of heterogeneous multi-task learning in the fashion domain. This problem can be well solved using our TSA, with an overall 4%~6% improvement (L5 vs. L7 and L6 vs. L8), even though only a few extra task-specific parameters are introduced (1.35% of the original CLIP size). Interestingly, we also found that XAA and TSA are reciprocal: (1) When TSA and XAA work together, the model can achieve better relative performance than the sum of their gains (L4 vs. L2+L3 and L8 vs. L6+L7) (2) When TSA or XAA is applied in isolation, the multi-task model always underperforms its single-task counterpart (L6 vs. L2 and L7 vs. L3). But the multi-task model with both TSA and XAA exceeds the single-task counterpart (L8 vs L4), indicating that TSA and XAA play complementary roles better in the multi-task setting, as expected and designed so.

4.3. Ablation study on multi-task training strategy

Following the above architecture analysis, we further ablate the proposed multi-teacher distillation (MTD) based training strategy. We compare extensively with previous sampling strategies and gradient manipulation algorithms.

Task sampling. We start by comparing two common sampling strategies (uniform and round-robin) with our size-proportional strategy. Round-robin sampling is a special case of uniform sampling – each task is sampled one by one. As shown in L9-L11 in the group (III) of Tab. 4, both uniform and round-robin sampling underperform our size-proportional sampling by a gap of 1.5%. This is due to imbalanced dataset sizes across different tasks, which is ignored in uniform sampling and round-robin sampling.

Gradient manipulation. To compare with our MTD scheme, we consider two kinds of gradient manipulation algorithms: Implicit Adaptive Scheduling (IAS) [32] and IMTLG [46]. In particular, IAS is a representative strong method that adaptively changes the task sampling ratio, learning rate, or gradient scale for each task [51, 80]. Specifically, it scales the gradients of each task according to the performance on the validation set. Instead, IMTLG is a representative of those methods manipulating all the gradients together [8, 36, 56, 63]. It is featured by a closed-form solution to optimize the scaling factors of each task, such that the aggregated gradients (sum of raw gradients weighted by the scaling factors) have equal projections onto individual tasks. Since IMTLG cannot be directly applied to task-sampling based MTL, we further adapt it by maintaining a gradient buffer to store the gradients of each task and update the parameters every four iterations (each corresponding one of the four fashion tasks). As shown in the group (III) of Tab. 4, the performance of IAS (L12) and IMTLG (L14) are significantly lower than that of our MTD (L9). In particular, IMTLG suffers from a severe negative transfer (-6.33%). There are two plausible reasons: (1) Relying on a heuristic strategy, IAS struggles in finding the optimal status over all tasks, despite the access to the validation performance. (2) IMTLG may experience over-fitting for the tasks with smaller training data (*e.g.*, TGIR), which cannot be addressed by the idea of ensuring the final gradient direction to have the same impact on each task. On the contrary, our MTD can implicitly regularize the gradients via knowledge distillation, without a costly need of monitoring the validation performance. Guided by the soft ground truth of each teacher, overfitting can be well avoided in an elegant manner. Considering the methodical orthogonality, we further apply our MTD on top of IAS (L13) and IMTLG (L15). It is shown that this can improve both by a large margin (L13 vs. L12 and L15 vs. L14), demonstrating the generic usability of our training method.

4.4. Further analysis

Regularizing effect of MTD. To shed more light on the regularization effect of MTD, we plot the validation performance curves in Fig. 5. Without MTD, the baseline MTL model is prone to overfit on TGIR after about 20k iterations due to much less training data than other tasks. Interestingly, this overfitting is even amplified by IMTLG. This is because IMTLG needs to pay more attention to TIRG in order to achieve impartial learning. Overall, neither IAS nor IMTLG can improve over the baseline MTL, regardless of overfitting or not. Encouragingly, our MTD yields consistent and significant performance boost per task, rendering it a more stable and effective learning strategy.

Scaling up bottleneck dimension. We evaluate the effect of the bottleneck dimension of the AdaptMLP in XAA

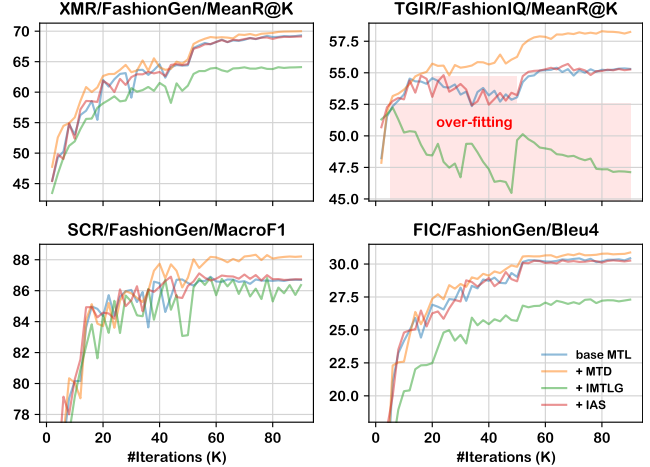


Figure 5. Training dynamics of our multi-teacher distillation (MTD) and alternative multi-task learning methods (IAS [32] and IMTLG [46]). Metric: The validation performance curves.

and TSA (the only hyper-parameter of our architecture). We vary this dimension from 64 to 512. As shown in the group (IV) of Tab. 4, it is evident that the overall relative performance is positively correlated with this bottleneck dimension. This indicates that FAME-ViL could be potentially more performing at the cost of more parameters. Also, we observe a trade-off between model size increase and performance gain. For example, 10% more parameters are needed for exchanging a relative performance gain of 1.4% (L18 vs. L9). We also notice that further improvement is not consistent over tasks. For instance, the performance of SCR will gradually deteriorate with the increase of bottleneck dimension. An interesting direction for future works could be exploiting adaptive algorithms [68, 69] to optimize the best bottleneck dimension per task.

Qualitative examples. To reflect the output of FAME-ViL more intuitively, in addition to Fig. 2, we show more illustrative outputs from FAME-ViL in the supplementary file.

5. Conclusions

We have introduced FAME-ViL for heterogeneous fashion tasks, grounded upon a generic off-the-shelf V+L model. It addresses cross-modal retrieval, text-guided image retrieval, multi-modal classification, and image captioning in a unified architecture. This is made possible by the proposed task-versatile architecture with cross-attention adapters and task-specific adapters, and a scalable multi-task training pipeline with multi-teacher distillation. Extensive experiments showed that our FAME-ViL achieves new state-of-the-art performance on all tasks with significantly fewer parameters.

Model architecture	Vision encoder (VE)	CLIP (ViT-B/16) [60]
	Language encoder (LE)	CLIP (ViT-B/16) [60]
	Bottleneck dim.	64
Data augmentation	Resize	(256, 256)
	RandomCrop	(224, 224)
	RandomHorizontalFlip	✓
Training setting	Number of iterations	90k
	Batch size	64
	Initial LR of VE/LE	1e-6
	Initial LR of Adapters	1e-4
	LR schedule	Multi-step
	LR steps	50k and 80k
	LR decrease ratio	0.1
	Warmup iterations	10k
	Warmup factor	0.25
	Optimizer	AdamW (0.9, 0.999)
Hardware	GPU	4 × RTX 3090
	Training duration	31.5h

Table 5. Details for multi-task training FAME-ViL.

A. Implementation details

This section describes our implementation and multi-task training details for FAME-ViL.

Architecture details. As mentioned in the main paper, we build our FAME-ViL upon off-the-shelf CLIP model [60]. We utilize the ViT-B/16 version and get the pre-trained weights from HuggingFace Transformers [82]. Specifically, as described in the original paper [60], the language encoder is a 12-layer 512-wide Transformer [73] with 8 attention heads, while the vision encoder is a base-size Vision Transformer (ViT) [17] with patch size as 16. Masked self-attention was used in the language encoder. For computational efficiency, the max text sequence length was capped at 76. The text sequence is bracketed with [SOS] and [EOS] tokens and the activations of the highest layer of the language encoder at the [EOS] token are treated as the text feature representation. Please find more details about CLIP and its pre-training in the original paper [60].

Training details. We list all hyper-parameters used for multi-task training in Tab. 5, including data augmentation methods, optimizer setting, scheduler setting, and *etc.* This results in about 31.5 hours of training time on four RTX 3090 GPUs (24GB memory for each). For single-task training (used by single-task teachers training and ablation study), we adopted the same hyper-parameters except for shorter training iterations (30k for tasks on Fashion-Gen [61], 6k for tasks on FashionIQ [83]).

B. Additional quantitative results

We followed the same protocol used by previous works [24] and used the same random seed for training, to ensure a direct comparison to these main competitors. We

(a) **Text query:** Satin cap in black. Adjustable snapback fastening. Tonal hardware. Tonal stitching.



(b) **Text query:** French terry lounge shorts in marled grey. Elasticized waistband. Three-pocket styling. Zip-fly.



(c) **Text query:** Wide-leg woven cotton sarouel-style trousers in dark navy. Partially elasticized waistband. Pleats at front. Two-pocket styling. Unlined.



(d) **Text query:** Relaxed-fit sweatshirt in heather grey. Ribbed knit crew-neck collar, cuffs, and hem. Raglan sleeves. Mock calf hair at breast in red.



(e) **Text query:** Short sleeve t-shirt in black. Rib-knit crew-neck collar. Logo printed at front in white and black. Tonal stitching.



Figure 6. XMR examples. Green box indicates the ground truth.

XMR* (Image to Text)			XMR* (Text to Image)		
R@1	R@5	R@10	R@1	R@5	R@10
45.99 ± 0.25	73.25 ± 0.15	81.84 ± 0.12	53.12 ± 0.07	77.55 ± 0.35	86.02 ± 0.22
TGIR (Dress)		TGIR (Shirt)		TGIR (Toptee)	
R@10	R@50	R@10	R@50	R@10	R@50
42.16 ± 0.32	67.10 ± 0.22	47.19 ± 0.33	67.91 ± 0.66	50.79 ± 0.08	73.48 ± 0.38
SCR (Acc)	SCR (F1)	FIC (B)	FIC (M)	FIC (R)	FIC (C)
94.62 ± 0.08	87.80 ± 0.25	30.59 ± 0.15	24.22 ± 1.99	55.69 ± 0.13	148.9 ± 1.19

Table 6. Statistical significance quantification of our results. * XMR evaluation is under full database protocol

also trained our model two more times with different random seeds to measure our method’s stability. The statistical performance (w/ mean and std) over three trials in Tab. 6 shows that our model is stable.

C. Additional qualitative results

We provide more visualization results in this section to better understand the performance of our FAME-ViL in a

(a) **Modifying text:** the shirt is purple and black, has slightly longer sleeves and is purple and black.



(b) **Modifying text:** is a green t-shirt with a light material, is more colorful.



(c) **Modifying text:** is blue with a collar and some buttons, is blue and shorter sleeved.



(d) **Modifying text:** is maroon with a ruffled top, is a dark red cowl-neck and long sleeves.



(e) **Modifying text:** is more plain and has tank top sleeves, is shorter and souped neck.



Figure 7. TGIR examples. Blue box indicates the reference image. Green box indicates the ground truth.

(a) **Text query:** Skinny-fit stretch denim jeans in 'fade to' grey. Fading and whiskering throughout. Mid-rise. Five-pocket styling.



(b) **Modify text:** is beige and sleeveless, is blue t-shirt with owls on front.



Figure 8. Failure cases. Blue box indicates the reference image. Green box indicates the ground truth.

qualitative way. Specifically, we show cross-modal retrieval (XMR) results in Fig. 6, text-guided image retrieval (TGIR) results in Fig. 7 and fashion image captioning (FIC) results in Tab. 7. We didn't show subcategory recognition (SCR)

Images	Ground Truth Captions	Generated Captions
(a)	White logo tank top. Relaxed-fit tank top in white. Ribbed scoopneck collar and armscyes. Logo print at black. Tonal logo embroidered at back hem. Tonal stitching.	White logo tank top. Racer-back tank top in white. Scoopneck collar. Logo printed at front in black. Curved hem. Tonal stitching.
(b)	Black python print shirt. Short sleeve shirt in tones of grey and black. Detailed python scale print throughout with ombre effect at bottom portions. Spread collar. Button closure at front. Tonal stitching. Single-button barrel cuffs with buttoned sleeve placket.	Black paint splatter shirt. Long sleeve shirt in black. Graphic print throughout in white. Spread collar. Button closure at front. Tonal stitching. Single-button barrel cuffs with buttoned sleeve placket.
(c)	Black jersey leather trim lounge pants. Leather-trimmed stretch jersey lounge pants in black. Partially elasticized waistband with leather drawstring closure. Zip fly. Leather pocket trim. Elasticized grosgrain cuffs.	Black lounge pants. Lounge pants in black. Elasticised waistband with drawstring closure. Four-pocket styling. Elasticised ankle cuffs. Tonal stitching. Zip fly.
(d)	Navy pixel print atari edition polo. Short sleeve oversized polo in navy. Atari pixel print at front. Spread collar with two-button placket. Slits at side seams. Tonal stitching.	Navy embroidered patch polo. Short sleeve cotton pique & eacute polo in navy. Ribbed spread collar and trim at sleeve opening. Five-button placket at front. Signature tri-color tab at back collar. Tennis tail hem. Tonal stitching.
(e)	Green wrap pencil skirt. High-waisted wrap pencil skirt in green. Gathered knot detail at waist. Vent at front hem. Zip closure at back. Tonal stitching.	Green silk draping skirt. Silk skirt in green. Elasticized waistband with drawstring at interior. Vented at back waist. Seam pockets at sides. Tonal stitching.

Table 7. FIC examples. Green text indicates the matched phrases.

results here because of the lack of intuition when visualizing this classification task, but the visualized attention maps are given in Fig. 9.

For retrieval tasks (XMR and TGIR), we observe ambiguities (*i.e.*, the ground truth is not the only one matching the query) in the fashion datasets [61, 83]. Especially in FashionIQ, there are many false negatives that are neglected during the data-annotation stage. Even so, our FAME-ViL can offer us a reliable and human-understandable ranking list, demonstrating its superiority in fine-grained discrimination. Fig. 8 shows example failure cases from (a) XMR and (b) TGIR. In the text query example, we can see that

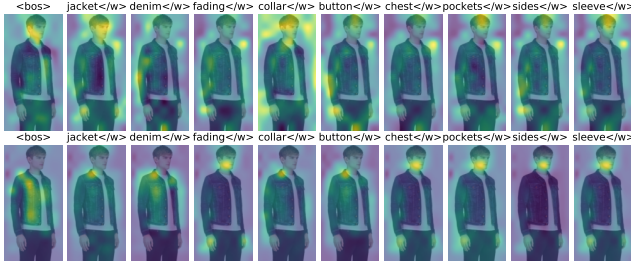


Figure 9. Visualized attention maps of SCR.

even the human-annotated ground truth (indicated by green boxes) images do not fit the text query perfectly. In both failure cases, the top retrieved results, though wrong according to the “ground truth”, are still largely aligned with the query/modify text.

Because of the fine-grained nature of the fashion domain, the ground truth captions in fashion contain much more fine-grained phrases than those in the generic domain [24]. Despite this challenge, our FAME-ViL can produce concrete and accurate phrases in the generated captions. Even if some of the generated phrases do not exist in the ground truth, they still conform to the content of the image and human intuition. This point proves the effectiveness of FAME-ViL in fine-grained generation.

To gain a more intuitive understanding of how attention is learned in our model, we visualize the *text-to-image attention maps* (the average over all heads) in the *last XAA* of the STL baseline (first row) and our MTL model (second row), as shown in Fig. 9. It is observed that the attention maps from our model are more accurate and meaningful.

References

- [1] Jimmy Lei Ba, Jamie Ryan Kiros, and Geoffrey E Hinton. Layer normalization. *arXiv preprint arXiv:1607.06450*, 2016. 3
- [2] Alberto Baldrati, Marco Bertini, Tiberio Uricchio, and Alberto Del Bimbo. Conditioned and composed image retrieval combining and partially fine-tuning clip-based features. In *CVPR workshops*, 2022. 2, 3, 4, 6
- [3] Alberto Baldrati, Marco Bertini, Tiberio Uricchio, and Alberto Del Bimbo. Effective conditioned and composed image retrieval combining clip-based features. In *CVPR*, 2022. 3
- [4] Satantjeet Banerjee and Alon Lavie. Meteor: An automatic metric for mt evaluation with improved correlation with human judgments. In *ACL workshops*, 2005. 5
- [5] Shoufa Chen, Chongjian Ge, Zhan Tong, Jiangliu Wang, Yibing Song, Jue Wang, and Ping Luo. Adaptformer: Adapting vision transformers for scalable visual recognition. In *NeurIPS*, 2022. 3, 4
- [6] Yanbei Chen, Shaogang Gong, and Loris Bazzani. Image search with text feedback by visiolinguistic attention learning. In *CVPR*, 2020. 2
- [7] Yen-Chun Chen, Linjie Li, Licheng Yu, Ahmed El Kholy, Faisal Ahmed, Zhe Gan, Yu Cheng, and Jingjing Liu. Uniter: Universal image-text representation learning. In *ECCV*, 2020. 1, 2, 3
- [8] Zhao Chen, Vijay Badrinarayanan, Chen-Yu Lee, and Andrew Rabinovich. Gradnorm: Gradient normalization for adaptive loss balancing in deep multitask networks. In *ICML*, 2018. 2, 3, 8
- [9] Zhe Chen, Yuchen Duan, Wenhai Wang, Junjun He, Tong Lu, Jifeng Dai, and Yu Qiao. Vision transformer adapter for dense predictions. *arXiv preprint arXiv:2205.08534*, 2022. 3
- [10] Patrick John Chia, Giuseppe Attanasio, Federico Bianchi, Silvia Terragni, Ana Rita Magalhães, Diogo Goncalves, Ciro Greco, and Jacopo Tagliabue. Fashionclip: Connecting language and images for product representations. *arXiv preprint arXiv:2204.03972*, 2022. 3
- [11] Kyunghyun Cho, Bart Van Merriënboer, Caglar Gulcehre, Dzmitry Bahdanau, Fethi Bougares, Holger Schwenk, and Yoshua Bengio. Learning phrase representations using rnn encoder-decoder for statistical machine translation. In *EMNLP*, 2014. 4
- [12] Kevin Clark, Minh-Thang Luong, Urvashi Khandelwal, Christopher D Manning, and Quoc Le. Bam! born-again multi-task networks for natural language understanding. In *ACL*, 2019. 2, 3, 5
- [13] Michael Crawshaw. Multi-task learning with deep neural networks: A survey. *arXiv preprint arXiv:2009.09796*, 2020. 2
- [14] Ginger Delmas, Rafael S Rezende, Gabriela Csurka, and Diane Larlus. Artemis: Attention-based retrieval with text-explicit matching and implicit similarity. In *ICLR*, 2022. 2
- [15] Jacob Devlin, Ming-Wei Chang, Kenton Lee, and Kristina Toutanova. BERT: Pre-training of deep bidirectional transformers for language understanding. In *NAACL-HLT*, 2019. 2
- [16] Eric Dodds, Jack Culpepper, and Gaurav Srivastava. Training and challenging models for text-guided fashion image retrieval. *arXiv preprint arXiv:2204.11004*, 2022. 3
- [17] Alexey Dosovitskiy, Lucas Beyer, Alexander Kolesnikov, Dirk Weissenborn, Xiaohua Zhai, Thomas Unterthiner, Mostafa Dehghani, Matthias Minderer, Georg Heigold, Sylvain Gelly, et al. An image is worth 16x16 words: Transformers for image recognition at scale. In *ICLR*, 2020. 2, 3, 6, 9
- [18] Zi-Yi Dou, Aishwarya Kamath, Zhe Gan, Pengchuan Zhang, Jianfeng Wang, Linjie Li, Zicheng Liu, Ce Liu, Yann LeCun, Nanyun Peng, et al. Coarse-to-fine vision-language pre-training with fusion in the backbone. In *NeurIPS*, 2022. 2, 4
- [19] Nanyi Fei, Zhiwu Lu, Yizhao Gao, Guoxing Yang, Yuqi Huo, Jingyuan Wen, Haoyu Lu, Ruihua Song, Xin Gao, Tao Xiang, et al. Towards artificial general intelligence via a multimodal foundation model. *Nature Communications*, 2022. 2
- [20] Robert M French. Catastrophic forgetting in connectionist networks. *Trends in cognitive sciences*, 1999. 3

- [21] Dehong Gao, Linbo Jin, Ben Chen, Minghui Qiu, Peng Li, Yi Wei, Yi Hu, and Hao Wang. Fashionbert: Text and image matching with adaptive loss for cross-modal retrieval. In *SIGIR*, 2020. 1, 3, 6
- [22] Sonam Goenka, Zhaoheng Zheng, Ayush Jaiswal, Rakesh Chada, Yue Wu, Varsha Hedau, and Pradeep Natarajan. Fashionvlp: Vision language transformer for fashion retrieval with feedback. In *CVPR*, 2022. 3, 6
- [23] Xiao Han, Sen He, Li Zhang, Yi-Zhe Song, and Tao Xiang. Uigr: Unified interactive garment retrieval. In *CVPR workshops*, 2022. 2
- [24] Xiao Han, Licheng Yu, Xiatian Zhu, Li Zhang, Yi-Zhe Song, and Tao Xiang. Fashionvil: Fashion-focused vision-and-language representation learning. In *ECCV*, 2022. 1, 2, 3, 4, 5, 6, 9, 11
- [25] Junxian He, Chunting Zhou, Xuezhe Ma, Taylor Berg-Kirkpatrick, and Graham Neubig. Towards a unified view of parameter-efficient transfer learning. In *ICLR*, 2022. 3, 4
- [26] Kaiming He, Xiangyu Zhang, Shaoqing Ren, and Jian Sun. Deep residual learning for image recognition. In *CVPR*, 2016. 6
- [27] Geoffrey Hinton, Oriol Vinyals, Jeff Dean, et al. Distilling the knowledge in a neural network. *arXiv preprint arXiv:1503.02531*, 2015. 5
- [28] Neil Houlsby, Andrei Giurgiu, Stanislaw Jastrzebski, Bruna Morroni, Quentin De Laroussilhe, Andrea Gesmundo, Mona Attariyan, and Sylvain Gelly. Parameter-efficient transfer learning for nlp. In *ICML*, 2019. 3
- [29] Edward J Hu, Yelong Shen, Phillip Wallis, Zeyuan Allen-Zhu, Yuanzhi Li, Shean Wang, Lu Wang, and Weizhu Chen. Lora: Low-rank adaptation of large language models. *arXiv preprint arXiv:2106.09685*, 2021. 3
- [30] Ronghang Hu and Amanpreet Singh. Unit: Multimodal multitask learning with a unified transformer. In *ICCV*, 2021. 3, 5
- [31] Zhicheng Huang, Zhaoyang Zeng, Yupan Huang, Bei Liu, Dongmei Fu, and Jianlong Fu. Seeing out of the box: End-to-end pre-training for vision-language representation learning. In *CVPR*, 2021. 2
- [32] Sébastien Jean, Orhan Firat, and Melvin Johnson. Adaptive scheduling for multi-task learning. *arXiv preprint arXiv:1909.06434*, 2019. 3, 7, 8
- [33] Ge-Peng Ji, Mingchen Zhuge, Dehong Gao, Deng-Ping Fan, Christos Sakaridis, and Luc Van Gool. Masked vision-language transformer in fashion. *Machine Intelligence Research*, 2022. 1, 3, 6
- [34] Chao Jia, Yinfei Yang, Ye Xia, Yi-Ting Chen, Zarana Parekh, Hieu Pham, Quoc Le, Yun-Hsuan Sung, Zhen Li, and Tom Duerig. Scaling up visual and vision-language representation learning with noisy text supervision. In *ICML*, 2021. 2
- [35] Menglin Jia, Luming Tang, Bor-Chun Chen, Claire Cardie, Serge Belongie, Bharath Hariharan, and Ser-Nam Lim. Visual prompt tuning. In *ECCV*, 2022. 3
- [36] Alex Kendall, Yarin Gal, and Roberto Cipolla. Multi-task learning using uncertainty to weigh losses for scene geometry and semantics. In *CVPR*, 2018. 2, 3, 8
- [37] Jongseok Kim, Youngjae Yu, Hoesong Kim, and Gunhee Kim. Dual compositional learning in interactive image retrieval. In *AAAI*, 2021. 2
- [38] Wonjae Kim, Bokyoung Son, and Ildoo Kim. Vilt: Vision-and-language transformer without convolution or region supervision. In *ICML*, 2021. 1, 2
- [39] Seungmin Lee, Dongwan Kim, and Bohyung Han. Cosmo: Content-style modulation for image retrieval with text feedback. In *CVPR*, 2021. 2
- [40] Junnan Li, Dongxu Li, Caiming Xiong, and Steven Hoi. Blip: Bootstrapping language-image pre-training for unified vision-language understanding and generation. In *ICML*, 2022. 4
- [41] Junnan Li, Ramprasaath Selvaraju, Akhilesh Gotmare, Shafiq Joty, Caiming Xiong, and Steven Chu Hong Hoi. Align before fuse: Vision and language representation learning with momentum distillation. In *NeurIPS*, 2021. 1, 2, 5
- [42] Liunian Harold Li, Mark Yatskar, Da Yin, Cho-Jui Hsieh, and Kai-Wei Chang. Visualbert: A simple and performant baseline for vision and language. *arXiv preprint arXiv:1908.03557*, 2019. 1, 2
- [43] Xiujuan Li, Xi Yin, Chunyuan Li, Pengchuan Zhang, Xiaowei Hu, Lei Zhang, Lijuan Wang, Houdong Hu, Li Dong, Furu Wei, et al. Oscar: Object-semantics aligned pre-training for vision-language tasks. In *ECCV*, 2020. 1, 2, 6
- [44] Lizi Liao, Xiangnan He, Bo Zhao, Chong-Wah Ngo, and Tat-Seng Chua. Interpretable multimodal retrieval for fashion products. In *ACM MM*, 2018. 1
- [45] Chin-Yew Lin. Rouge: A package for automatic evaluation of summaries. In *ACL workshops*, 2004. 5
- [46] Liyang Liu, Yi Li, Zhanghui Kuang, Jing-Hao Xue, Yimin Chen, Wenming Yang, Qingmin Liao, and Wayne Zhang. Towards impartial multi-task learning. In *ICLR*, 2020. 2, 3, 7, 8
- [47] Pengfei Liu, Weizhe Yuan, Jinlan Fu, Zhengbao Jiang, Hiroaki Hayashi, and Graham Neubig. Pre-train, prompt, and predict: A systematic survey of prompting methods in natural language processing. *arXiv preprint arXiv:2107.13586*, 2021. 3
- [48] Zheyuan Liu, Cristian Rodriguez-Opazo, Damien Teney, and Stephen Gould. Image retrieval on real-life images with pre-trained vision-and-language models. In *ICCV*, 2021. 1, 6
- [49] Jiasen Lu, Dhruv Batra, Devi Parikh, and Stefan Lee. Vilbert: Pretraining task-agnostic visiolinguistic representations for vision-and-language tasks. In *NeurIPS*, 2019. 1, 2, 4
- [50] Jiasen Lu, Christopher Clark, Rowan Zellers, Roozbeh Mottaghi, and Aniruddha Kembhavi. Unified-io: A unified model for vision, language, and multi-modal tasks. *arXiv preprint arXiv:2206.08916*, 2022. 2
- [51] Jiasen Lu, Vedanuj Goswami, Marcus Rohrbach, Devi Parikh, and Stefan Lee. 12-in-1: Multi-task vision and language representation learning. In *CVPR*, 2020. 3, 8
- [52] Haoyu Ma, Handong Zhao, Zhe Lin, Ajinkya Kale, Zhangyang Wang, Tong Yu, Jiuxiang Gu, Sunav Choudhary, and Xiaohui Xie. Ei-clip: Entity-aware interventional contrastive learning for e-commerce cross-modal retrieval. In *CVPR*, 2022. 2, 3, 4, 6

- [53] Yihui Ma, Jia Jia, Suping Zhou, Jingtian Fu, Yejun Liu, and Zijian Tong. Towards better understanding the clothing fashion styles: A multimodal deep learning approach. In *AAAI*, 2017. 1
- [54] Yuning Mao, Lambert Mathias, Rui Hou, Amjad Almahairi, Hao Ma, Jiawei Han, Scott Yih, and Madian Khabsa. Unipelt: A unified framework for parameter-efficient language model tuning. In *ACL*, 2022. 3
- [55] Suvir Mirchandani, Licheng Yu, Mengjiao Wang, Animesh Sinha, Wenwen Jiang, Tao Xiang, and Ning Zhang. Fad-vlp: Fashion vision-and-language pre-training towards unified retrieval and captioning. In *EMNLP*, 2022. 3
- [56] Aviv Navon, Aviv Shamsian, Idan Achituve, Haggai Maron, Kenji Kawaguchi, Gal Chechik, and Ethan Fetaya. Multi-task learning as a bargaining game. In *ICML*, 2022. 2, 3, 8
- [57] Duy-Kien Nguyen and Takayuki Okatani. Multi-task learning of hierarchical vision-language representation. In *CVPR*, 2019. 3
- [58] Kishore Papineni, Salim Roukos, Todd Ward, and Wei-Jing Zhu. Bleu: a method for automatic evaluation of machine translation. In *ACL*, 2002. 5
- [59] Adam Paszke, Sam Gross, Francisco Massa, Adam Lerer, James Bradbury, Gregory Chanan, Trevor Killeen, Zeming Lin, Natalia Gimelshein, Luca Antiga, et al. Pytorch: An imperative style, high-performance deep learning library. In *NeurIPS*, 2019. 5
- [60] Alec Radford, Jong Wook Kim, Chris Hallacy, Aditya Ramesh, Gabriel Goh, Sandhini Agarwal, Girish Sastry, Amanda Askell, Pamela Mishkin, Jack Clark, et al. Learning transferable visual models from natural language supervision. In *ICML*, 2021. 1, 2, 3, 9
- [61] Negar Rostamzadeh, Seyedarian Hosseini, Thomas Boquet, Wojciech Stokowiec, Ying Zhang, Christian Jauvin, and Chris Pal. Fashion-gen: The generative fashion dataset and challenge. *arXiv preprint arXiv:1806.08317*, 2018. 1, 2, 3, 4, 5, 6, 9, 10
- [62] Victor Sanh, Thomas Wolf, and Sebastian Ruder. A hierarchical multi-task approach for learning embeddings from semantic tasks. In *AAAI*, 2019. 5
- [63] Ozan Sener and Vladlen Koltun. Multi-task learning as multi-objective optimization. In *NeurIPS*, 2018. 2, 3, 8
- [64] Minchul Shin, Yoonjae Cho, Byungsoo Ko, and Geonmo Gu. Rtic: Residual learning for text and image composition using graph convolutional network. *arXiv preprint arXiv:2104.03015*, 2021. 2
- [65] Amanpreet Singh, Vedanuj Goswami, Vivek Natarajan, Yu Jiang, Xinlei Chen, Meet Shah, Marcus Rohrbach, Dhruv Batra, and Devi Parikh. Mmf: A multimodal framework for vision and language research. <https://github.com/facebookresearch/mmf>, 2020. 5
- [66] Amanpreet Singh, Ronghang Hu, Vedanuj Goswami, Guillaume Couairon, Wojciech Galuba, Marcus Rohrbach, and Douwe Kiela. Flava: A foundational language and vision alignment model. In *CVPR*, 2022. 2, 3
- [67] Weijie Su, Xizhou Zhu, Yue Cao, Bin Li, Lewei Lu, Furu Wei, and Jifeng Dai. VL-BERT: pre-training of generic visual-linguistic representations. In *ICLR*, 2020. 1, 2
- [68] Benyuan Sun, Jin Dai, Zihao Liang, Congying Liu, Yi Yang, and Bo Bai. Gppf: A general perception pre-training framework via sparsely activated multi-task learning. *arXiv preprint arXiv:2208.02148*, 2022. 8
- [69] Ximeng Sun, Rameswar Panda, Rogerio Feris, and Kate Saenko. Adashare: Learning what to share for efficient deep multi-task learning. In *NeurIPS*, 2020. 8
- [70] Yi-Lin Sung, Jaemin Cho, and Mohit Bansal. VI-adapter: Parameter-efficient transfer learning for vision-and-language tasks. In *CVPR*, 2022. 3
- [71] Ilya Sutskever, Oriol Vinyals, and Quoc V Le. Sequence to sequence learning with neural networks. In *NeurIPS*, 2014. 4
- [72] Hao Tan and Mohit Bansal. LXMERT: Learning cross-modality encoder representations from transformers. In *EMNLP-IJCNLP*, 2019. 1, 4
- [73] Ashish Vaswani, Noam Shazeer, Niki Parmar, Jakob Uszkoreit, Llion Jones, Aidan N. Gomez, Lukasz Kaiser, and Illia Polosukhin. Attention is all you need. In *NeurIPS*, 2017. 2, 3, 9
- [74] Ramakrishna Vedantam, C Lawrence Zitnick, and Devi Parikh. Cider: Consensus-based image description evaluation. In *CVPR*, 2015. 5
- [75] Nam Vo, Lu Jiang, Chen Sun, Kevin Murphy, Li-Jia Li, Li Fei-Fei, and James Hays. Composing Text and Image for Image Retrieval - an Empirical Odyssey. In *CVPR*, 2019. 2, 4, 6
- [76] Jianfeng Wang, Xiaowei Hu, Zhe Gan, Zhengyuan Yang, Xiyang Dai, Zicheng Liu, Yumao Lu, and Lijuan Wang. Ufo: A unified transformer for vision-language representation learning. *arXiv preprint arXiv:2111.10023*, 2021. 2
- [77] Peng Wang, An Yang, Rui Men, Junyang Lin, Shuai Bai, Zhikang Li, Jianxin Ma, Chang Zhou, Jingren Zhou, and Hongxia Yang. Ofa: Unifying architectures, tasks, and modalities through a simple sequence-to-sequence learning framework. In *ICML*, 2022. 2
- [78] Wenhui Wang, Hangbo Bao, Li Dong, Johan Bjorck, Zhiliang Peng, Qiang Liu, Kriti Aggarwal, Owais Khan Mohammed, Saksham Singhal, Subhojit Som, et al. Image as a foreign language: Beit pretraining for all vision and vision-language tasks. *arXiv preprint arXiv:2208.10442*, 2022. 2
- [79] Wenhui Wang, Hangbo Bao, Li Dong, and Furu Wei. Vlm0: Unified vision-language pre-training with mixture-of-modality-experts. *arXiv preprint arXiv:2111.02358*, 2021. 1, 2
- [80] Weiyao Wang, Du Tran, and Matt Feiszli. What makes training multi-modal classification networks hard? In *CVPR*, 2020. 8
- [81] Ronald J Williams and David Zipser. A learning algorithm for continually running fully recurrent neural networks. *Neural computation*, 1989. 4
- [82] Thomas Wolf, Lysandre Debut, Victor Sanh, Julien Chaumond, Clement Delangue, Anthony Moi, Pierric Cistac, Tim Rault, Rémi Louf, Morgan Funtowicz, Joe Davison, Sam Shleifer, Patrick von Platen, Clara Ma, Yacine Jernite, Julien Plu, Canwen Xu, Teven Le Scao, Sylvain Gugger, Mariama

- Drame, Quentin Lhoest, and Alexander M. Rush. Transformers: State-of-the-art natural language processing. In *EMNLP*, 2020. 5, 9
- [83] Hui Wu, Yupeng Gao, Xiaoxiao Guo, Ziad Al-Halah, Steven Rennie, Kristen Grauman, and Rogerio Feris. Fashion iq: A new dataset towards retrieving images by natural language feedback. In *CVPR*, 2021. 1, 2, 4, 5, 6, 9, 10
- [84] Xiao Xu, Chenfei Wu, Shachar Rosenman, Vasudev Lal, and Nan Duan. Bridge-tower: Building bridges between encoders in vision-language representation learning. *arXiv preprint arXiv:2206.08657*, 2022. 2
- [85] Xuewen Yang, Heming Zhang, Di Jin, Yingru Liu, Chi-Hao Wu, Jianchao Tan, Dongliang Xie, Jue Wang, and Xin Wang. Fashion captioning: Towards generating accurate descriptions with semantic rewards. In *ECCV*, 2020. 1, 2, 3, 4
- [86] Jiahui Yu, Zirui Wang, Vijay Vasudevan, Legg Yeung, Mojtaba Seyedhosseini, and Yonghui Wu. Coca: Contrastive captioners are image-text foundation models. *arXiv preprint arXiv:2205.01917*, 2022. 2, 4
- [87] Licheng Yu, Jun Chen, Animesh Sinha, Mengjiao MJ Wang, Hugo Chen, Tamara L Berg, and Ning Zhang. Commercem: Large-scale commerce multimodal representation learning with omni retrieval. In *KDD*, 2022. 1, 3
- [88] Pengchuan Zhang, Xiujun Li, Xiaowei Hu, Jianwei Yang, Lei Zhang, Lijuan Wang, Yejin Choi, and Jianfeng Gao. Vinvl: Revisiting visual representations in vision-language models. In *CVPR*, 2021. 2
- [89] Yuanhan Zhang, Kaiyang Zhou, and Ziwei Liu. Neural prompt search. *arXiv preprint arXiv:2206.04673*, 2022. 3
- [90] Yida Zhao, Yuqing Song, and Qin Jin. Progressive learning for image retrieval with hybrid-modality queries. In *SIGIR*, 2022. 6
- [91] Kaiyang Zhou, Jingkang Yang, Chen Change Loy, and Ziwei Liu. Conditional prompt learning for vision-language models. In *CVPR*, 2022. 3
- [92] Kaiyang Zhou, Jingkang Yang, Chen Change Loy, and Ziwei Liu. Learning to prompt for vision-language models. *IJCV*, 2022. 3
- [93] Luowei Zhou, Hamid Palangi, Lei Zhang, Houdong Hu, Jason Corso, and Jianfeng Gao. Unified vision-language pre-training for image captioning and vqa. In *AAAI*, 2020. 6
- [94] Mingchen Zhuge, Dehong Gao, Deng-Ping Fan, Linbo Jin, Ben Chen, Haoming Zhou, Minghui Qiu, and Ling Shao. Kaleido-bert: Vision-language pre-training on fashion domain. In *CVPR*, 2021. 1, 2, 3, 4, 5, 6